Original Contribution

NADPH oxidase 4 regulates homocysteine metabolism and protects against acetaminophen-induced liver damage in mice

CrossMark

Thomas V.A. Murray [a], Xuebin Dong [a], Greta J. Sawyer [a], Anna Caldwell [b], John Halket [b], Roy Sherwood [c], Alberto Quaglia [d], Tracy Dew [c], Narayana Anilkumar [a], Simon Burr [a], Rajesh K. Mistry [a], Daniel Martin [a], Katrin Schröder [e], Ralf P. Brandes [e], Robin D. Hughes [d], Ajay M. Shah [a], Alison C. Brewer [a],*

[a] Cardiovascular Division, King's College London, 125 Coldharbour Lane, London E5 0AD
[b] Mass Spectrometry Facility, King's College London, FWB, 150 Stamford Street London E1 9NH
[c] NHS Foundation Trust, King's College Hospital, Denmark Hill, London SE5 9RS
[d] Institute of Liver Studies, King's College London, Denmark Hill, London SE5 9RS
[e] Institut für Kardiovaskuläre Physiologie, Goethe-Universität, 60596 Frankfurt am Main, Germany

ARTICLE INFO

ABSTRACT

Glutathione is the major intracellular redox buffer in the liver and is critical for hepatic detoxification of xenobiotics and other environmental toxins. Hepatic glutathione is also a major systemic store for other organs and thus impacts on pathologies such as Alzheimer's disease, Sickle Cell Anaemia and chronic diseases associated with aging. Glutathione levels are determined in part by the availability of cysteine, generated from homocysteine through the transsulfuration pathway. The partitioning of homocysteine between remethylation and transsulfuration pathways is known to be subject to redox-dependent regulation, but the underlying mechanisms are not known. An association between plasma Hcy and a single nucleotide polymorphism within the NADPH oxidase 4 locus led us to investigate the involvement of this reactive oxygen species- generating enzyme in homocysteine metabolism. Here we demonstrate that NADPH oxidase 4 ablation in mice results in increased flux of homocysteine through the betaine-dependent remethylation pathway to methionine, catalysed by betaine-homocysteine-methyltransferase within the liver. As a consequence NADPH oxidase 4-null mice display significantly *lowered* plasma homocysteine and the flux of homocysteine through the transsulfuration pathway is reduced, resulting in lower hepatic cysteine and glutathione levels. Mice deficient in NADPH oxidase 4 had markedly increased susceptibility to acetaminophen-induced hepatic injury which could be corrected by administration of N-acetyl cysteine. We thus conclude that under physiological conditions, NADPH oxidase 4-derived reactive oxygen species is a regulator of the partitioning of the metabolic flux of homocysteine, which impacts upon hepatic cysteine and glutathione levels and thereby upon defence against environmental toxins.

1. Introduction

The term "oxidative stress" has become synonymous with a plethora of seemingly unrelated pathological conditions. Central to this concept is the fact that an overproduction of free radicals, including reactive oxygen and nitrogen species (ROS and RNS) which are produced in many physiological processes, results in the damage of macromolecular cell components [31]. Production of these damaging oxidants is buffered by the maintenance of a complex array of antioxidant systems, of which the most abundant is the tripeptide glutathione (γ-glutamylcysteineylglycine; GSH) redox system [39]. GSH is synthesized within all cells from glycine,

cysteine and glutamate by the enzymatic actions of γ-gluta-mylcysteine ligase (GCL) and glutathione synthetase (GS), and is consumed in the detoxification of harmful electrophilic metabolites and xenobiotics. Depletion of intracellular GSH is taken as an indicator of oxidative stress, and is implicated in the pathogenesis of diverse disease states including Systemic Lupus Erythematosus, Oedematous Protein Energy Malnutrition, central nervous system disorders such as Alzheimer's disease, Sickle Cell Anaemia and chronic diseases associated with aging and infection [39,43].

The most significant site of GSH production is the liver [53]. GSH is present at very high concentrations (5–10 mM) in hepatocytes, and is central to the predominant role played by the liver in the metabolism of xenobiotics. In addition, the liver is the major exporter of GSH [22] and, as a consequence, a depletion of GSH within the liver has particularly profound systemic clinical effects [49].

The intracellular cysteine pool is relatively small and many studies have demonstrated that it is the limiting amino acid for GSH synthesis in humans [29], and increasing the supply of cysteine prevents GSH deficiency under several pathological conditions [28,49]. Cysteine can be imported directly into cells, or is produced via metabolism of Homocysteine (Hcy).

Hcy is synthesised endogenously from methionine and lies at the intersection of two metabolic pathways whereby it can be remethylated to methionine or metabolised to cysteine by transsulfuration (Fig. 1). Approximately 50% of cysteine needed for hepatic GSH production comes via this transsulfuration pathway [33], which involves sequential enzymatic activities of cysthathionine β-synthase (CBS) and cystathionine γ-lyase (CGL). Accordingly, perturbations in this pathway can affect GSH production, as illustrated by the phenotype of CBS-null mice in which GSH levels are severely compromised [51]. Hcy can alternatively be remethylated to methionine by two pathways. One is folate-dependent and is catalysed by methionine synthase (MS) using 5-methyltetrahydrofolate as the methyl donor [14]. The second occurs exclusively in liver and (less so) in kidney, and is catalysed by the enzyme betaine-homocysteine-methyltransferase (BHMT) using betaine as the methyl donor [14].

Partitioning of Hcy through the transsulfuration and remethylation metabolic pathways is redox-regulated. Thus the activities of three of the major Hcy metabolising enzymes; MS, BHMT and CBS, are regulated by specific redox-dependent protein modifications [23]. Intriguingly, the enzymes involved in remethylation pathways are inhibited by pro-oxidants whereas the activity of CBS is increased. Furthermore, in human hepatocytes in vitro there is a linear correlation between the concentration of exogenous oxidant added and the production of cysteine via transsulfuration [33]. However, the relevant endogenous oxidant source(s) which mediate this remains unknown.

Perturbations in Hcy metabolism are reflected by altered levels of circulating plasma Hcy concentrations which correlate with a diverse range of pathologies including vascular dysfunction, neurodegenerative disorders, congenital defects and diabetes, together with renal and hepatic syndromes [40]. These variations in plasma Hyc levels are highly heritable. However, apart from some rare mutations, the underlying genetic determinants remain unknown [35]. In a genome-wide association analysis (GWAS), single-nucleotide polymorphisms (SNPs) in genes that associate with plasma Hcy concentration were identified. In addition to genes whose functions have already been associated with Hcy metabolism, associations with four novel gene loci were identified, one of which was NADPH oxidase 4 (Nox4) [35].

The NADPH oxidase family of enzymes are important generators of intracellular ROS which modulate redox-dependent signalling pathways. There are 7 Nox isoforms identified in mammals (Nox1–5 and Duox1/2) which show specificity of cellular distribution, intracellular location, mechanisms of action and types of ROS produced [4]. Nox4 has been shown to produce predominantly H_2O_2 [47], and is widely expressed in many cell types and adult tissues including kidney, liver, heart and aorta [24]. Given the known role of redox regulation of Hcy metabolic pathways and the association of Nox4 with hyperhomocysteinemia, a potential regulatory role for Nox4 in Hcy metabolism could be inferred. To address this, we studied the plasma Hcy levels in a Nox4-null (Nox4$^{-/-}$) mouse model. We show that Nox4 ablation significantly promotes the metabolic flux of Hcy along the folate-independent remethylation pathway resulting in significantly decreased total plasma Hcy levels. This further impinges on the transsulfuration pathway leading to significantly decreased cysteine production and hepatic GSH stores. As a consequence, Nox4$^{-/-}$ mice display markedly increased susceptibility to acetaminophen (APAP, paracetamol)-induced hepatoxicity.
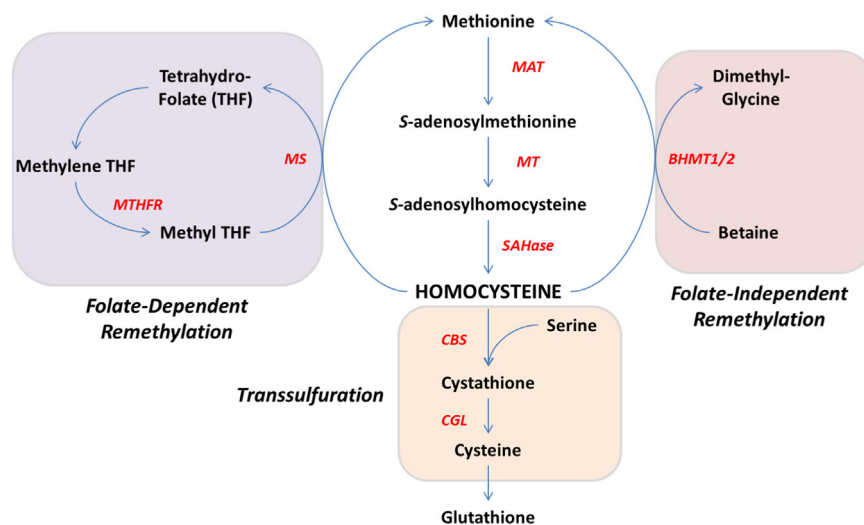

Fig. 1. Schematic representation of Hcy metabolism. Hcy lies at the crossroads of remethylation and transsulfuration pathways. MS: methionine synthase, MT: methyltransferase, MAT: methionine-adenosyltransferase, BHMT: betaine-homocysteine-methyltransferase, SAHase: S-adenosylhomocysteine-hydrolase, CBS: cystathione-β-synthase, CGL: cystathione-γ-lyase.

2. Materials and Methods

Animals-Nox4$^{-/-}$ mice have been described previously [54]. Mice were fed *ad libitum* on standard chow or folate-deficient/ respective control diets (Harlan, [27]) as described. APAP (200 mg/ kg) and N-acetylcysteine (NAC, 500 mg/kg; both Sigma) were administered by oral gavage. For APAP rescue experiments NAC (10 mg/ml) was additionally added to mouse drinking water 24hours prior to APAP/NAC gavage. Blood was harvested by cardiac puncture. All experimental procedures were performed following protocols approved by the ethical committee of King's College London in accordance with the UK Animals (Scientific) Procedures Act of 1986.

2.1. Metabolic Cage Study

8-week-old female mice were fasted overnight and subsequently housed in metabolic cages for 6hours, during which time they were not given food but had free access to water. Urine collected was snap frozen in liquid nitrogen until analysed.

2.2. Western Blot

Protein samples were prepared from homogenised tissue, separated on SDS-PAGE gels, transferred to membranes and probed with appropriate antibodies as described previously [34]. Antibodies used: β-Actin (Sigma), BHMT (Abcam).

RNA analyses: RNA preparation from cell culture and tissue, cDNA generation and QPCR were all performed as described previously [6]. Primer sets used to detect mouse transcripts were as follows (5' to 3'): *β-actin* F: CTGTCGAGTCGCGTCCACCC, R: ATGCCGGAGCCGTTGTCGAC; *MS* F: GCAGATGTGGCCAGAAAAG, R: GCCACAAACCTCTTGACTCC; *MTHFR* F: GAAGAACATAATGGCGCTG AG, R: GGCATAGCTGAAGCCTCCTT; *BHMT* F: GACAAGCTGGAAAA-CAGAGGA, R: GACAAGCTGGAAAACAGAGGA; *choline dehydrogenase* F: TGTCTGGAAGTCCCAGTGC, R: GAAGCAGGACTGCACCATTC; *MAT1A* F: CATCGTGCTCGCTCACAAAC, R: CACCAGAGCGCCTCAGATC; *MAT2A* F: TTACGCCCAGATTCTAAAACTCAA, R: GCACAGCACCCCGATCTT; *MAT2B* F: CTGCTTCCCAGCTGAATGTG, R: TCGCAGCTGCCTC-CTTTG. Primers used to detect human transcripts were: *β-actin* F: GCGAGAAGATGACCGAGATCA, R: TCACCGGAGTCCATCAC-GAT, *choline dehydrogenase* F: GTGCACCGTATCCTGTCACT, R: TCTGATCCACGGAGGGGAAT, *BHMT* F: TCACCTTCTATGCGAGTGAAGA, R: CAAGCAGCTTCATTGACTTCC.

2.3. Glutathione Measurements on liver tissue

Freshly isolated liver tissue was snap-frozen in liquid N$_2$, and stored at − 80 °C until analysed. Samples were homogenised in phosphate-buffered saline containing 2 mM EDTA, at a concentration of 25 mg tissue/ml PBS, and subsequently diluted 1/10 in PBS/EDTA for analyses. GSH assays were performed using the GSH-Glo assay kit (Promega), according to manufacturer's recommendations with modifications as described previously [6]. To measure total GSH levels (GSH+GSSG) extracts (50 µl) were pre-incubated in a fixed concentration of 1 mM Tris(2-carbox-yethylphosphine hydrochloride (TCEP; Sigma) for 30minutes at room temperature. From measurements of total and reduced GSH the level of oxidized GSSG, and the glutathione redox couple (GSH: GSSG) were calculated. It should be noted that this method typically results in higher levels of total GSH than described elsewhere in the literature, and as a consequence the GSH:GSSG ratios are routinely lower than described by others. We believe this to be due to the very strong reducing power of the TCEP, and as its effect is consistent across all samples, it in no way invalidates the relative values presented here.

2.4. Methionine and Cysteine Measurements in Liver samples

For methionine measurements liver tissue was homogenised in ice-cold 5% percholoric acid, centrifuged and the supernatant (extract) collected. Methionine was measured in extracts from Wt and Nox4$^{-/-}$ mouse livers using a Bridge-It® L-Methionine (L-Met) Fluorescence Assay (mediomics) as per the manufacturer's protocol. Cysteine content was determined using a previously described method [16].

ALT and AST Activity Measurements-Plasma samples were analysed using an ADVIA 2400 Chemistry System (Siemens Healthcare Diagnostics.

Homocysteine Measurements-Hcy concentrations were determined in plasma and urine using the ADVIA Centaur CP Immunoassay System (Siemens Healthcare Diagnostics Ltd.).

2.6. Histology and Assessment of Liver Injury

Sections of the right medial lobe of the liver were harvested and fixed in 4% paraformaldehyde for 4hours at 4 °C. Sections were dehydrated stepwise in graded concentrations of ethanol and embedded in paraffin. 6 µm sections were stained with haematoxylin and eosin (H&E) for light microscopic examination using an Olympus BH51 microscope. Pictures were taken using an Olympus DP26 digital camera. Sections were reviewed and graded by a liver histopathologist (AQ) blind to genotype and treatment conditions. An initial review of the sections identified three significant features of histological injury; hepatocellular ballooning, presence of sinusoidal congestion, and confluent hepatocellular necrosis. After careful search at 200x or 400x magnification sections were subsequently graded as follows: none visible: No abnormalities apparent in liver sections, grade 1: no necrosis, minimal sinusoidal congestion with some hepatocellular ballooning present, grade 2: no necrosis, moderate sinusoidal congestion and hepatocellular ballooning, grade 3: focal necrosis limited to the area immediately around the centrilobular vein, moderate sinusoidal congestion and hepatocellular ballooning, grade 4: marked necrosis around the centrilobular vein and extending into the midzonal cell region (coagulative-type hepatocellular necrosis) presenting as a diffuse change, immediately evident at low power magnification, and affecting more than one third of the lobular area), panlobular congestion and significant hepatocellular ballooning.

2.7. Measurement of Hepatic Betaine and Dimethylglycine

Liver samples or HepG2 cells were harvested, snap frozen and stored until analysed. Tissue samples and cells were homogenised in acetonitrile containing 0.1% formic acid (185 µl/20 mg tissue). 100 µl of extract was evaporated to dryness and resuspended in a solution of 0.1% pentafluorooctanoic acid, 0.1% formic acid in 0.5% acetonitrile in water containing 50 ng/ml of Pemoline as an internal standard and vortexed to mix. Samples were analysed on a Thermo Accela LC system interfaced directly to Thermo LTQ XL linear ion trap mass spectrometer.

2.8. Immunocytochemistry

HepG2 cells were cultured on cover slips, before fixation (4% paraformaldehyde, 15minutes) and permeabilisation (0.1% triton X-100 in PBS, 20minutes). After blocking (3% BSA, 1.5% normal goat serum in PBS), cells were incubated with primary antibodies against BHMT (mouse monoclonal, ab52144, AbCam, 1:500 dilution) and Nox4 (rabbit polyclonal; 1:200 dilution [1]. Antibody bindings were visualised using Alexa 568-conjugated anti-mouse IgG and 488-conjugated anti-rabbit IgG secondary antibodies

(Invitrogen Molecular Probes; 1:200 dilution). Images were visualised using a Leica scanning confocal microscope (TCS-SP5). Red and green fluorescent signals were detected using appropriate filter sets (excitation 568/emission 620 nm or 488/emission 505–530 nm respectively). Confocal images were acquired as transcellular 0.4 μm sections in the Z plane (15 scans/plane).

2.9. Quantatative Analyses of Co-localisation

Co-localisation of BHMT and Nox4 staining was quantified using the ImageJ: Coloc2 plugin (National Institutes of Health), in order to calculate the Pearson's correlation coefficient, which gives a measure of the correlation between the intensity distributions of the red (BHMT) and green (Nox4) channels. 5 independent, unsaturated images were used for the analysis.

2.10. Glutathione assays on HepG2 cells

HepG2 cells were seeded (10^4 cells/well) on a 96-well cell culture plate that had been coated with a 1% gelatin solution. Cells were transduced with an adenovirus vector encoding either Nox4 (AdNox4) or β-galactosidase (AdβGal) as control at an MOI of 20. Cells were incubated for 24 h and GSH assays were performed using the GSH-Glo assay kit (Promega), according to manufacturer's recommendations.

2.11. Measurement of ROS

Catalase-Inhibitable extracellular ROS, generated by HepG2 cells (transduced with AdNox4/AdβGal, as above) cells was measured using a homovanillic acid- (HVA-)based assay, as described previously [2].

2.12. BIAM-labeling

Labeling of BHMT protein was carried out essentially as described previously [42]. All buffers were deoxygenated by bubbling with argon gas for at least 30 mins. 300 ng of purified BHMT (Abcam) or BSA (Sigma) were used per reaction, in labelling buffer (100 mM phosphate buffer, pH 6.0, 50 mM NaCl, 1 mM EDTA, 1 mM EGTA). Protein was treated with H_2O_2 for 20mins with concentrations as indicated, or with 20 mM N-ethyl-maleimide (NEM; Sigma), before incubation with 10 μM N-(biotinoyl)-N'-(iodoacetyl) ethylenediamine (BIAM; Life Technologies) at 37 °C for 30 mins. The labeling reaction was stopped by the addition of 20 mM DTT (final concentration). BIAM-labeled proteins were affinity purified on magnetic streptavidin-coated beads (Dyna beads) and analysed by immunoblotting.

For direct labelling of BHMT in HepG2 cells (transduced with AdNox4/AdβGal, as above), the 'BIAM Switch' method [8] was used. Briefly, HepG2 cells were incubated with 20 mM NEM, 30 mins, at 37 C. Cells were then washed with ice cold PBS to remove excess NEM. Cells were lysed in labelling buffer containing 0.5% NP-40 and protein was quantitated by Bradford assy. 300 ug total protein was used per sample. Oxidised residues were reduced by the addition of DTT to a final concentration of 3 mM. Excess DTT was removed using Zeba™ Spin Desalting Columns, 7 K MWCO (Thermo, cat. No. 89882) and then labelled with 10uM BIAM, 37 C, 30mins. The reaction was stopped by the addition of 20 mM DTT. BIAM labelled proteins were affinity purified on magnetic streptavidin-coated beads (Dyna beads). Labelled proteins were analysed by immunoblot.

Statistics-Data are expressed as mean ± S.E. Comparisons between sample groups or measurements at different time points were made by unpaired Student's t test.

3. Results

3.1. Nox4 deficiency decreases plasma levels of Hcy

We investigated the effect of Nox4 deficiency on plasma Hcy concentrations. 8-week-old female wild-type (Wt) and Nox4$^{-/-}$ mice were fed a normal chow diet *ad libitum* or were fasted overnight after which total plasma Hcy concentrations were determined. Feeding/fasting had no significant effect on baseline plasma Hcy levels (Fig. 2A). However, a highly significant *reduction* in plasma Hcy concentration was observed in Nox4$^{-/-}$ mice compared to Wt mice, irrespective of feeding status (Fig. 2A). A similar result was obtained using cohorts of 8-week-old (fasted) male mice (Fig. 2A), indicating that the effect of Nox4 ablation on plasma Hcy concentrations is not sex-dependent. Since baseline concentrations of Hcy differ between male and female mice in general [51], all subsequent experiments were performed on female mice for consistency.

Altered renal function has been associated with altered plasma Hcy levels [15]. Since Nox4 is highly expressed in the kidney [17], renal Hcy clearance was determined. Urine production, and creatinine excretion and clearance rates were similar in both sets of animals (Fig. 2B,C&D.). Excretion rates of Hcy were significantly lower in the Nox4$^{-/-}$ cohort (as expected due to the lower plasma Hcy concentrations; Fig. 2E), however there were no differences in Hcy clearance rates between the two groups (Fig. 2F). Thus renal function of Nox4$^{-/-}$ animals is comparable to that of Wt controls.

3.2. Cysteine and GSH levels are reduced in Nox4$^{-/-}$ mouse livers

Cysteine is generated from Hcy, predominantly in the liver, *via* the transsulfuration pathway (Fig. 3A) and its bioavailability critically affects levels of hepatic GSH [46]. Therefore we measured hepatic cysteine and GSH levels and found that cysteine levels, GSH levels and the GSH/GSSG ratio were all significantly reduced in Nox4$^{-/-}$ liver samples (Fig. 3B,C&D).

To determine whether the lower GSH levels were due to the reduced hepatic cysteine levels, mice were injected with either vehicle or 500 mg/kg of N-acetyl cysteine (NAC) for 4hours before livers were harvested. NAC treatment restored GSH levels (Fig. 3E) and normalised the GSH:GSSG ratio of Nox4$^{-/-}$ mice to that of Wt control animals (Fig. 3F). We therefore propose that lower bioavailability of cysteine due to reduced Hcy flux through the transsulfuration pathway is the underlying cause of the low hepatic GSH levels in the Nox4$^{-/-}$ mice.

3.3. Nox4$^{-/-}$ animals are more susceptible to liver damage in a model of acetaminophen (APAP)-induced hepatotoxicity

Decreased antioxidant capacity has been linked to increased susceptibility to hepatotoxic agents. Therefore we tested whether the Nox4$^{-/-}$ mice were more susceptible to APAP-induced hepatotoxicity. Wt and Nox4$^{-/-}$ mice were fasted overnight and subsequently administered either vehicle or a moderate dose of APAP (200 mg/kg, oral gavage) which was shown previously not to induce significant mortality ($< 10\%$) within a 24 h period [44]. After 24hours mice were sacrificed and the activities of the liver enzymes alanine-transaminase (ALT) and aspartate-transaminase (AST) in blood plasma were determined. Baseline activity levels were equivalent in the two groups, and Wt APAP-treated animals showed no significant change in these enzymatic activity levels compared to vehicle-treated controls. However, Nox4$^{-/-}$ animals exhibited highly significant and strikingly increased AST and ALT activity levels upon APAP treatment, consistent with substantial liver damage (Fig. 4A&B).
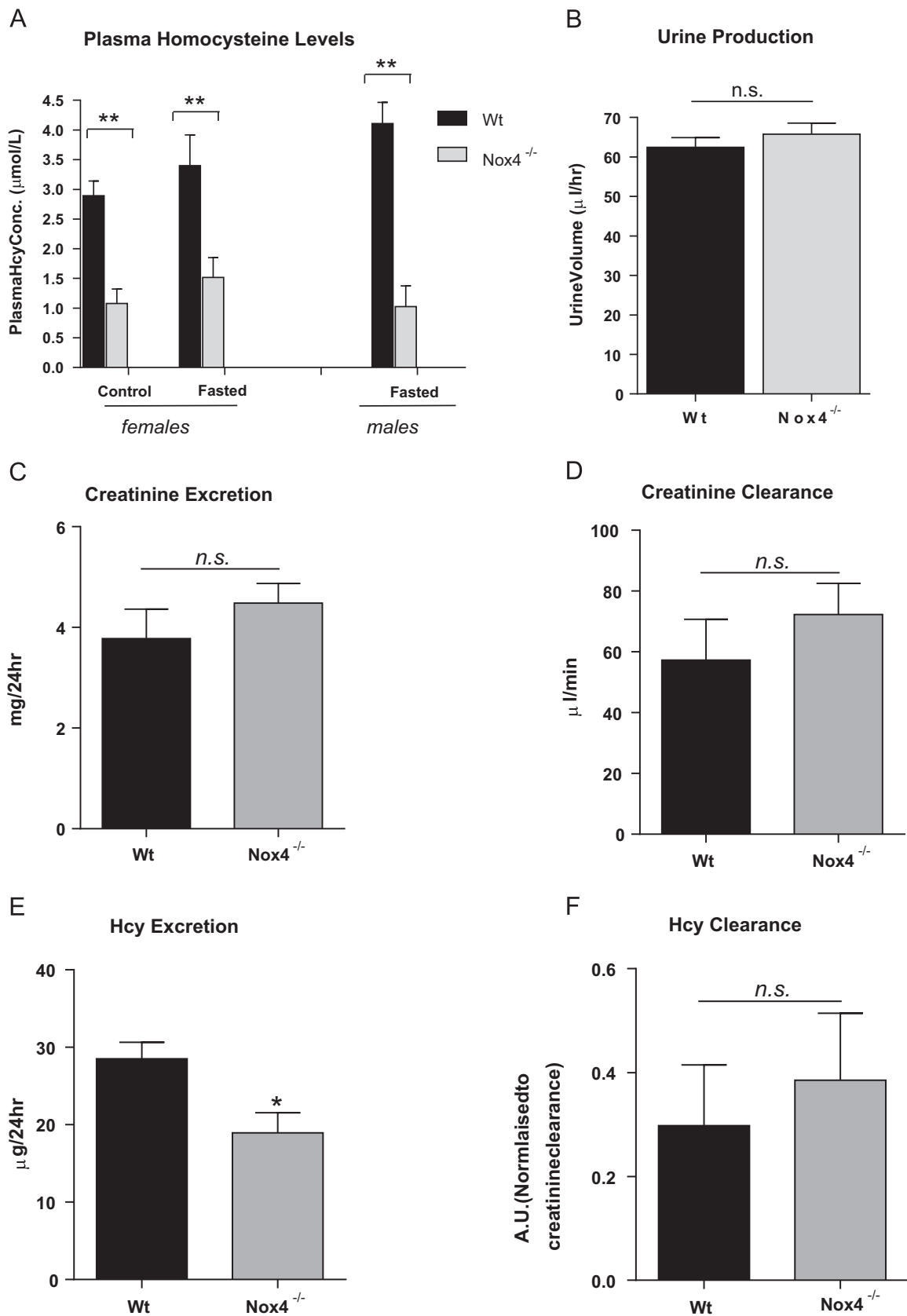
Fig. 2. *Ablation of Nox4 decreased plasma levels of Hcy.* Plasma Hcy concentrations in A, fed (control) or fasted 8-week-old female Wt and Nox4$^{-/-}$ mice (n=5) and fed 8-week-old male Wt and Nox4$^{-/-}$ mice (n=3). B, Urine production from Wt and Nox4$^{-/-}$ mice (n=3 groups of 5). C, Creatinine excretion rates (CERs) of Wt and Nox4$^{-/-}$ mice (n=3 groups of 5). D, Creatinine clearance rates (CCRs) levels in Wt and Nox4$^{-/-}$ mice (n=4). E, Hcy excretion rates (HERs) in Wt and Nox4-/- mice (n=3 groups of 5). F, Hcy clearance rates normalised to CCRs, in Wt and Nox4$^{-/-}$ mice (n=4). All data are presented as mean +/-S.E.M. **: p= < 0.01. *: p= < 0.05. n.s.: not significant.
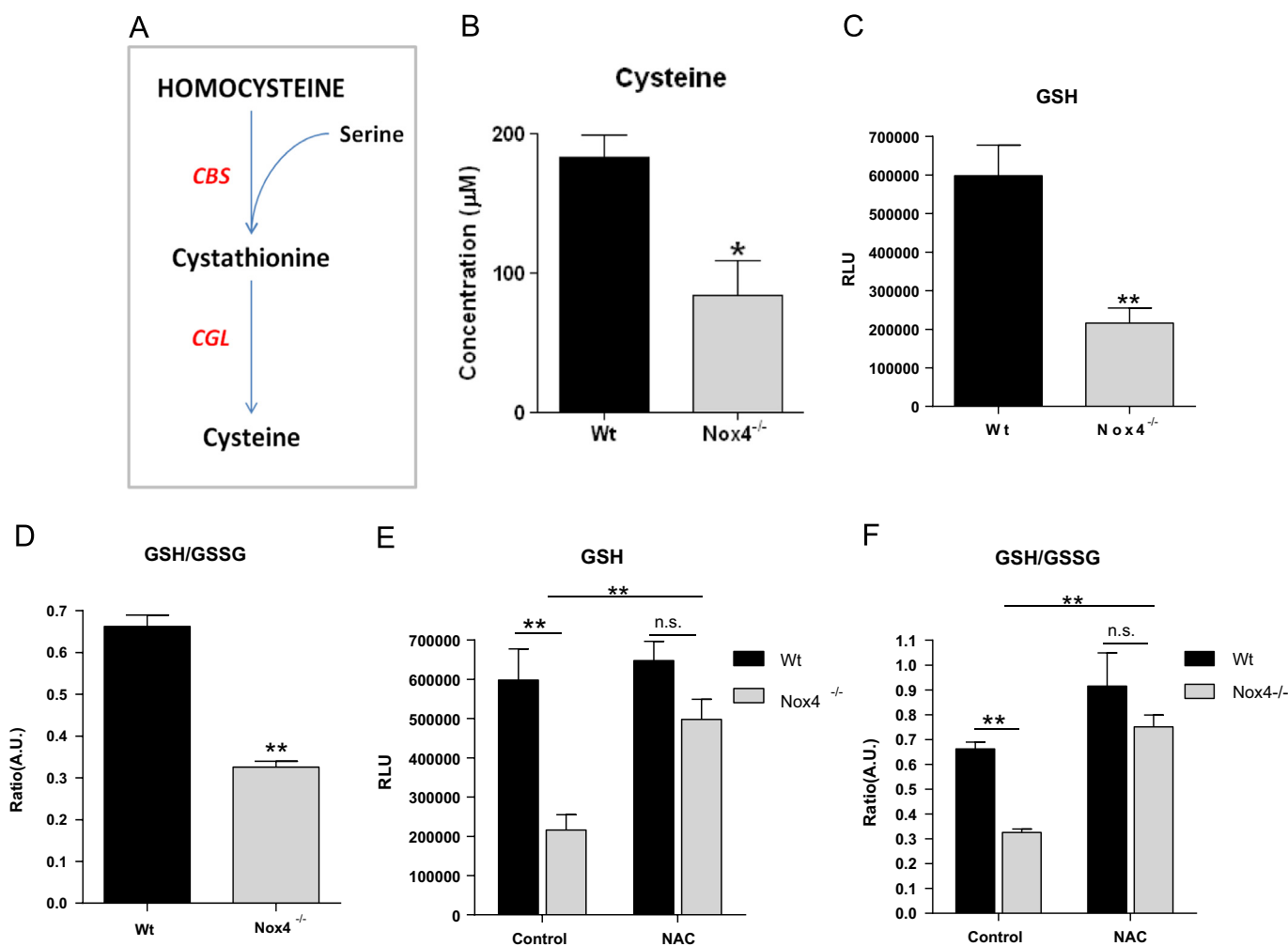
Fig. 3. *Lower Hcy levels in Nox4$^{-/-}$ mice resulted in reduced hepatic levels of cysteine and GSH.*A, Schematic representation of the endogenous transsulfuration pathway (CBS: cystathionine β-synthase, CGL: cystathionine gamma-lyase). B, Cysteine concentration, C, Level of glutathione (GSH) and D, Ratio of GSH/GSSG in liver extracts from 8-week-old female Wt and Nox4$^{-/-}$ liver homogenates (n=5). E, Level of GSH in 8-week old female Wt and Nox4-/- liver homogenates assessed 4hours after administration of either saline (control) or NAC (500 mg/kg; n=3). F, Ratio of GSH/GSSG in samples as in E. RLU; Relative light units. AU: Arbitary scale. All data are presented as mean +/-S.E.M. **: p= < 0.01. *: p= < 0.05. n.s.: not significant.

Liver sections from control Wt and Nox4$^{-/-}$ mice exhibited normal histology with no signs of damage at baseline (Fig. 4C), while those from Wt mice treated with APAP presented with only mild histological signs of injury. Thus they displayed some sinusoidal congestion and hepatocellular ballooning (arrowed in Fig. 4D&F (Wt)) but without confluent necrosis in centrilobular and perivenular areas. By contrast, and consistent with the significantly elevated activity levels of AST and ALT, Nox4$^{-/-}$ mice treated with APAP exhibited severe liver damage. In these animals, areas of confluent necrosis were apparent in a pattern typical of APAP overdosage [37] that was accompanied by pronounced sinusoidal congestion and significant hepatocyte ballooning injury (arrowed in Fig. 4D&F (Nox4$^{-/-}$)). Apoptosis has been shown to occur after APAP overdose [37], and accordingly substantially more apoptotic bodies were observed in liver sections from Nox4$^{-/-}$ mice which were primarily associated with areas of frank necrosis. Co-administration of NAC (both 10 mg/ml from previous 24hours in drinking water, together with 500 mg/kg by oral gavage) with APAP to both Wt and Nox4$^{-/-}$ mice remarkably reversed most of the damage associated with APAP treatment in both groups as evidenced by decreased ALT and AST activity levels (Fig. 4A&B), and by the inhibition of hepatocellular injury markers. Most notably, NAC treatment completely protected against hepatocellular necrosis in Nox4$^{-/-}$ animals (Fig. 4E). Thus ablation of Nox4 renders mice

significantly more susceptible to APAP-induced hepatotoxicity, primarily due to reduced hepatic cysteine, and hence decreased GSH levels. These results are summarized in Table 1.

3.4. Folate-dependent remethylation is not compromised in Nox4$^{-/-}$ mice

Our data suggest that lower Hcy levels in Nox4$^{-/-}$ mice impact upon the flux of Hcy to cysteine, resulting in reduced GSH levels and increased susceptibility to hepatotoxic agents. As Nox4 is known to be an important generator of physiological levels of ROS, we sought to identify redox-dependent mechanism(s) which might underlie this reduction in Hcy levels. The remethylation of Hcy to methionine by both folate-dependent and –independent mechanisms is known to be inhibited by oxidation [23], thus Nox4 ablation might potentially *increase* the activity of either or both of these pathways. The folate-dependent remethylation pathway, catalysed by MS (Fig. 5A), can be inhibited by dietary folate deprivation, resulting in increased plasma Hcy levels [7]. Wt and Nox4-/- mice were therefore fed a folate-deficient diet. As expected, Wt plasma Hcy levels increased significantly within 2 days of folate deprivation and remained significantly higher at 2 weeks (Fig. 5B). By contrast, plasma Hcy levels of the Nox4$^{-/-}$ mice did *not* increase with folate deprivation at either time-point (Fig. 5B). Thus
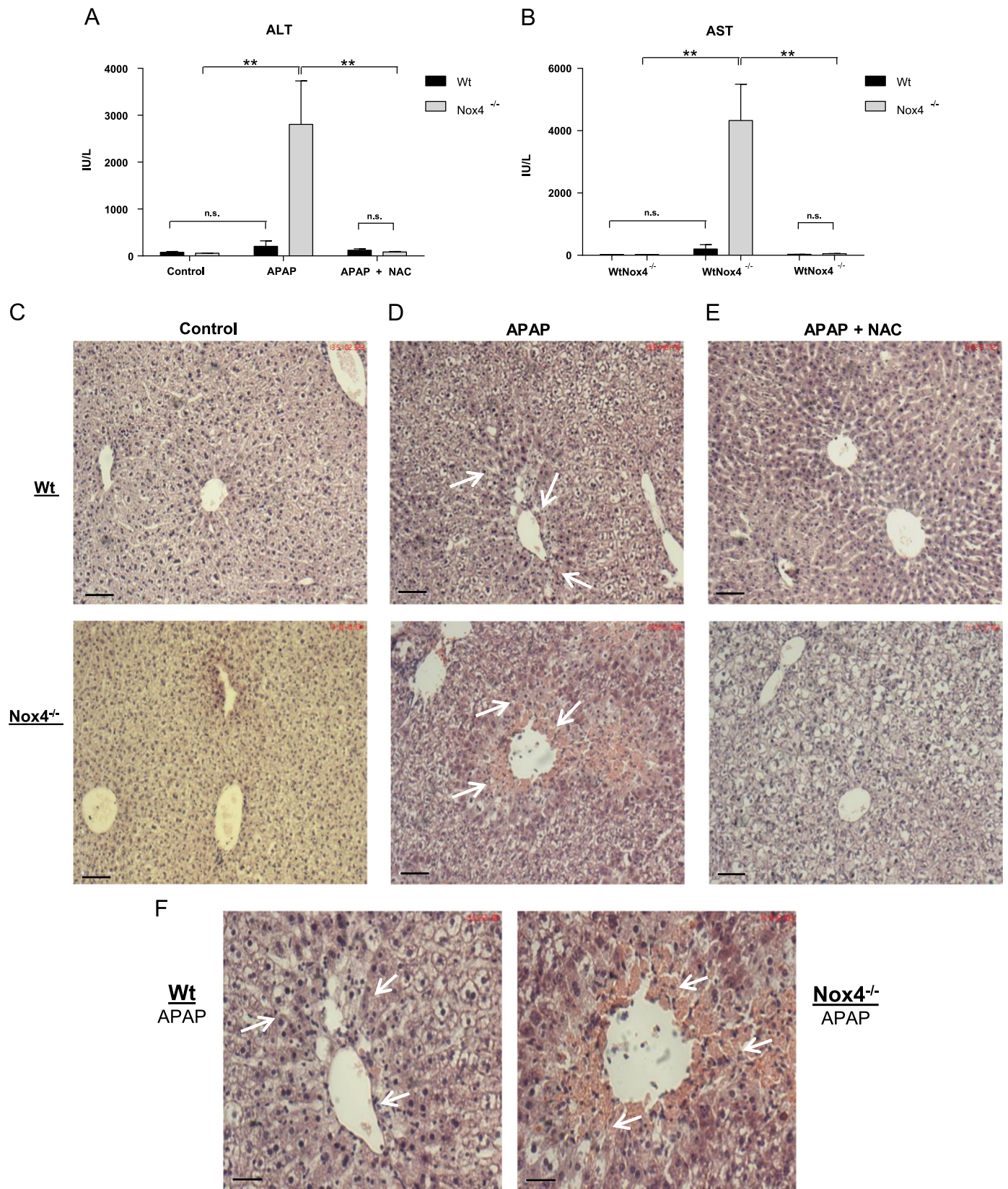
Fig. 4. *Nox4$^{-/-}$ animals are more susceptible to liver damage in a model of acetaminophen-induced hepatotoxicity.*Wt and Nox4$^{-/-}$ (n=5 in each group) mice were fasted overnight, followed by administration of either water (control), acetaminophen (APAP; 200 mg/kg) or APAP+NAC (200 mg/kg and 500 mg/kg respectively). After 24hours mice were sacrificed and plasma and tissue samples were harvested. A & B, Aminotransferase activity assays of ALT and AST activity respectively in plasma from Wt and Nox4-/- animals after treatments as indicated. IU/L: standard international units per litre. C, D, and E: H & E stained histological sections of liver from Wt and Nox4-/- mice after treatments as indicated Scale bar: 70 μm. F, Higher magnification images of sections shown in D. Scale bar 17 μm. All data are presented as mean +/-S.E.M. **: p= < 0.01. n.s.: not significant. (Arrows depict areas of hepatocellular ballooning, sinusoidal congestion and necrosis.).

Table 1

Grading of liver injury after APAP treatment: Animals received 300 mg APAP/kg. NAC was administered at 500 mg/kg. The degree of ballooning, necrosis and congestion were graded according to the criteria outlined in materials and methods. n=5 per group. Highly significant changes in all criteria were observed in the Nox4$^{-/-}$ cohort, compared to all other groups**: p= < 0.01 vs Wt. Data presented as Mean $\pm$ SEM.

	Hepatocellular Ballooning	Confluent Necrosis	Congestion
Wt Saline	none visible	none visible	none visible
Nox4$^{-/-}$ Saline	none visible	none visible	none visible
Wt APAP	2.0 ± 0.20	0.75 ± 0.02	0.35 ± 0.15
Nox4$^{-/-}$ APAP	2.6 ± 0.30**	3.75 ± 0.09**	1.0 ± 0.19**
Wt APAP NAC	0.25 ± 0.06	none visible	none visible
Nox4$^{-/-}$ APAP NAC	0.60 ± 0.03	none visible	none visible

the cause of the lower Hcy levels in Nox4$^{-/-}$ mice is *not* due to increased flux through the folate-dependent remethylation pathway since inhibition of this pathway served only to increase the difference in plasma Hcy levels between Wt and Nox4$^{-/-}$ mice.

3.5. Nox4 ablation increases hepatic betaine homocysteine methyltransferase (BHMT)-catalysed remethylation

The folate independent remethylation of Hcy to methionine, catalysed by BHMT, uses betaine as the methyl donor (Fig. 6A). Betaine is exclusively and irreversibly catabolised by BHMT to generate dimethylglycine (DMG) [36], and the ratio of the hepatic concentration of betaine:DMG can be taken as a measure of the activity of this pathway [13,21,32]. We therefore determined the concentrations of BHMT and DMG in liver samples from Wt and Nox4$^{-/-}$ mice by mass spectrometry. Liver betaine concentrations were significantly lower in the Nox4$^{-/-}$ mouse cohort (Fig. 6B) while their DMG levels were similar to those of livers from Wt mice (Fig. 6C). We calculated the ratio of DMG:betaine and demonstrated a highly significant decrease in this ratio in the Nox4$^{-/-}$ mice, indicative of increased BHMT-mediated remethylation (Fig. 6D). Hepatic BHMT mRNA (Fig. 6E) and protein (Fig. 6F) *expression* levels were unchanged between Wt and Nox4$^{-/-}$ mice. These data are therefore consistent with a redox-mediated increase in BHMT metabolic *activity*, resulting from Nox4 ablation, acting to lower both liver betaine levels and plasma levels of Hcy.

Changes in betaine bioavailablity have been suggested to be linked causally to changes in choline dehydrogenase (CDH; which

catalyses betaine biosynthesis) mRNA expression [12]. Perhaps consistent with this, mRNA levels of CDH were significantly increased in Nox4$^{-/-}$ liver samples (Fig. 6G). However protein levels of CDH were not determined in this previous study, and we were unable to determine any difference between CDH protein expression in Nox4$^{-/-}$ and wt livers (data not shown). The significance of these observations therefore remains unclear.

3.6. The Nox4-dependent regulation of BHMT activity is a conserved mechanism in human HepG2 cells

To investigate further the mechanism of Nox4-dependent regulation of BHMT *in vitro*, we utilised the HepG2 human hepatocyte cell line. We immunostained HepG2 cells for Nox4 and BHMT. Consistent with previous observations we saw strong Nox4 expression in the nucleus [1], in addition to diffuse extra-nuclear expression, while BHMT expression was predominantly extra-nuclear (Fig. 7F). Pearson correlation coefficient analysis demonstrated a negative correlation of Nox4 and BHMT within the nuclear compartment, but significant co-localisation outside of the nucleus (Fig. 7F). Adenoviral-mediated overexpression of Nox4 in HepG2 cells resulted in significantly higher intracellular levels of betaine (Fig. 7A) and GSH (Fig. 7B), consistent with redox-dependent *inhibition* of BHMT, and complementary to our *in vivo* observations. The mRNA and protein levels of BHMT were unchanged by Nox4 overexpression (Fig. 7C & D); again consistent with a post-translational redox-dependent regulatory mechanism. There was also a statistically significant, albeit small, decrease in CDH mRNA levels upon Nox4 overexpression, again complimentary to our *in vivo* observations (Fig. 7E).

Crystal structure analyses of BHMT have demonstrated a potential structural basis for a functional switch in BHMT activity, dependent upon the oxidation of critical cysteine residues which co-ordinate a zinc ion within its active site [10]. We sought to determine whether BHMT is a *bona fide* target of H_2O_2-mediated oxidation. Recombinant BHMT was incubated with increasing concentrations of H_2O_2 and its oxidation status was assessed using N-(biotinoyl)-N'-(iodoacetyl) ethylenediamine (BIAM), which irreversibly alkylates reduced thiol (S-H) groups. Thus a reduction in BIAM incorporation reflects an *increase* in unlabelled cysteine residues which are susceptible to H_2O_2-mediated oxidation. Western blot analyses revealed a dose-dependent susceptibility of BHMT to H_2O_2-induced oxidation at physiological concentrations (< 20 μM) [9]. By contrast, under equivalent experimental conditions, BSA was oxidised only at relatively high (non-physiological) concentrations of H_2O_2 (> 100 μM) (Fig. 8A&B).
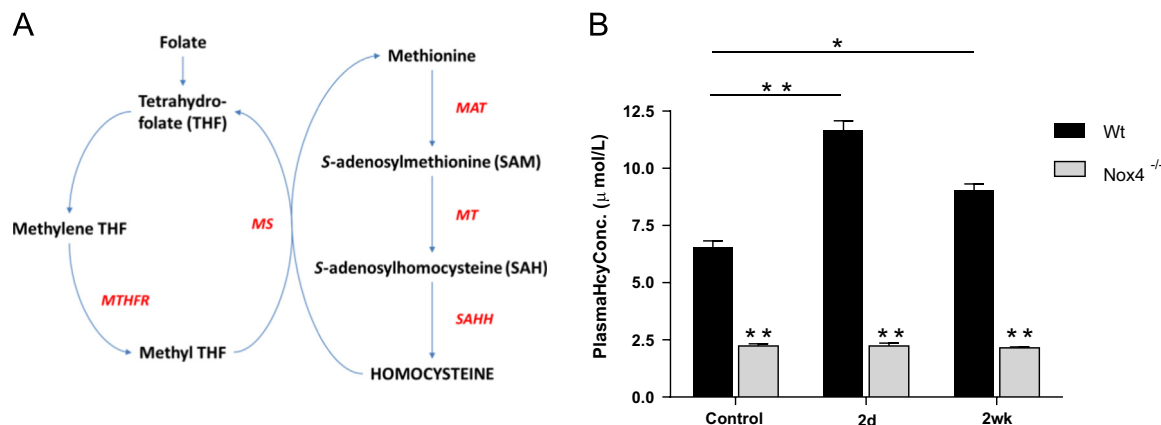

Fig. 5. *Lower plasma Hcy levels were not due to increased folate-dependent remethylation*. A, Schematic representation of endogenous Hcy biosynthetic and folate-dependent remethylation pathways. (MAT: methionine adenosyltransferase, MT: methyl transferases, SAHH: *S*-adenosylhomocysteine hydrolase, MS: methionine synthase, MTHFR: methyltetrahydrofolate reductase). B, Plasma Hcy concentrations from Wt and Nox4$^{-/-}$ mice fed a folate-deficient or control diet for time points as indicated (n=5). All data are presented as mean +/-S.E.M. **: p= < 0.01. *: p= < 0.05. n.s.: not significant.
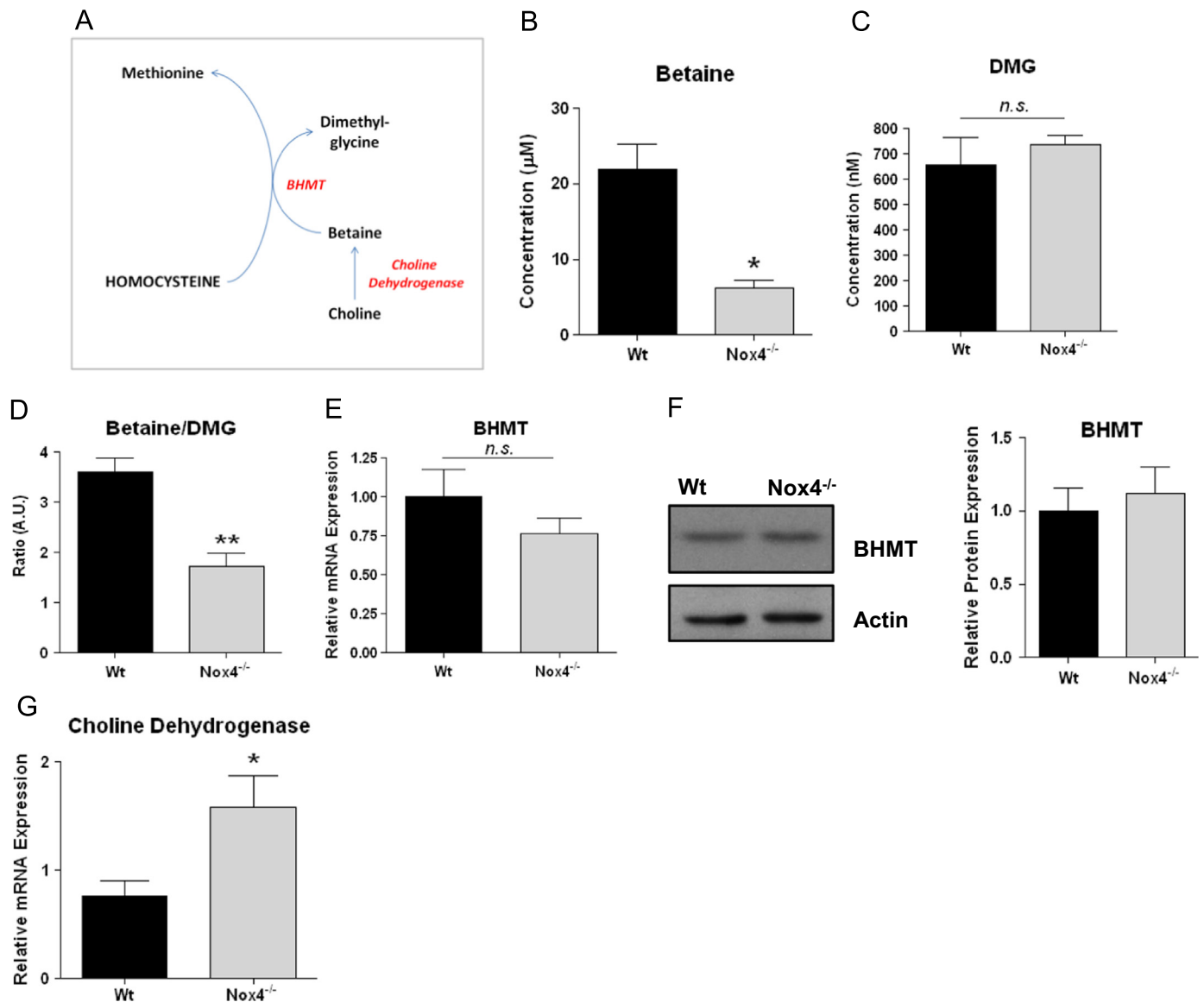
Fig. 6. *Nox4 ablation increased hepatic betaine homocysteine methyltransferase (BHMT)-catalysed remethylation.*A, Schematic representation of the endogenous folate-*independent* remethylation pathway (BHMT: betaine homocysteine methyltransferase). B,C,D Quantification of mass spectrometry analyses of extracts from 8 week old female Wt and Nox4$^{-/-}$ liver samples to determine concentrations of betaine (B) dimethylglycine (DMG; C) and ratio of betaine: DMG (D; n=3 in each case). E, Q-PCR analysis of BHMT mRNA expression in 8 week old female Wt and Nox4$^{-/-}$ liver samples, relative to levels of β-actin (n=5). F, Representative immunoblot and quantitative histogram indicating BHMT protein expression levels in liver samples from 8 week old female Wt and Nox4$^{-/-}$ mice (n=3). G, Q-PCR analysis of choline dehydrogenase mRNA expression levels in liver samples from 8 week old female Wt and Nox4$^{-/-}$ mice relative to levels of β-actin (n=3). All data are presented as mean +/-S.E.M. **: p= < 0.01. *: p= < 0.05. n.s.: not significant.

Nox4 is known to generate H_2O_2 specifically. Accordingly, overexpression of Nox4 in HepG2 cells resulted in a significant increase in catalase-inhibitable extracellular H_2O_2 (Fig. 8C), consistent with our previous studies in HEK293 cells and HUVECs [2,38]. Therefore, to test whether Nox4 overexpression, *per se*, induced BHMT oxidation, a direct, "biotin-switch" labelling strategy was employed [8]. As shown (Fig. 8D), Nox4 overexpression in HepG2 cells induced a highly significant increase in labelled (and hence oxidised) BHMT, consistent with the increased susceptibility of the recombinant protein to H_2O_2-induced oxidation, described above. Therefore, taken together, these results suggest that BHMT activity can potentially be regulated by direct redox-regulation of critical cysteine residues *via* Nox4-generated H_2O_2.

4. Discussion

Here we report that the total plasma concentrations of Hcy in Nox4$^{-/-}$ mice are profoundly reduced irrespective of sex or nutritional status. In addition our data clearly demonstrate that the lower basal levels of plasma Hcy result in reduced metabolic flux to cysteine, and consequently lower hepatic GSH levels. This is of significant clinical importance, since depleted GSH stores have far-reaching implications for disease susceptibility and progression, as exemplified by the strikingly increased sensitivity of Nox4$^{-/-}$ mice to APAP-induced hepotoxicity that we observe here.

Although Nox4 is highly expressed within the kidney [17], we found no evidence that altered renal Hcy clearance in the Nox4$^{-/-}$ mice accounts for the lowered plasma Hcy levels,consistent with a previous study, which found no detectable kidney dysfunction at baseline in Nox4$^{-/-}$ mice [3]. We therefore conclude that the hypohomocystenemia observed in Nox4$^{-/-}$ mice was due to the dysregulation of systemic Hcy metabolism.

Hcy is predominantly metabolised in the liver [46]. Our data strongly support the premise that the flux of Hcy through the remethylation or transsulfuration pathways is under redox-
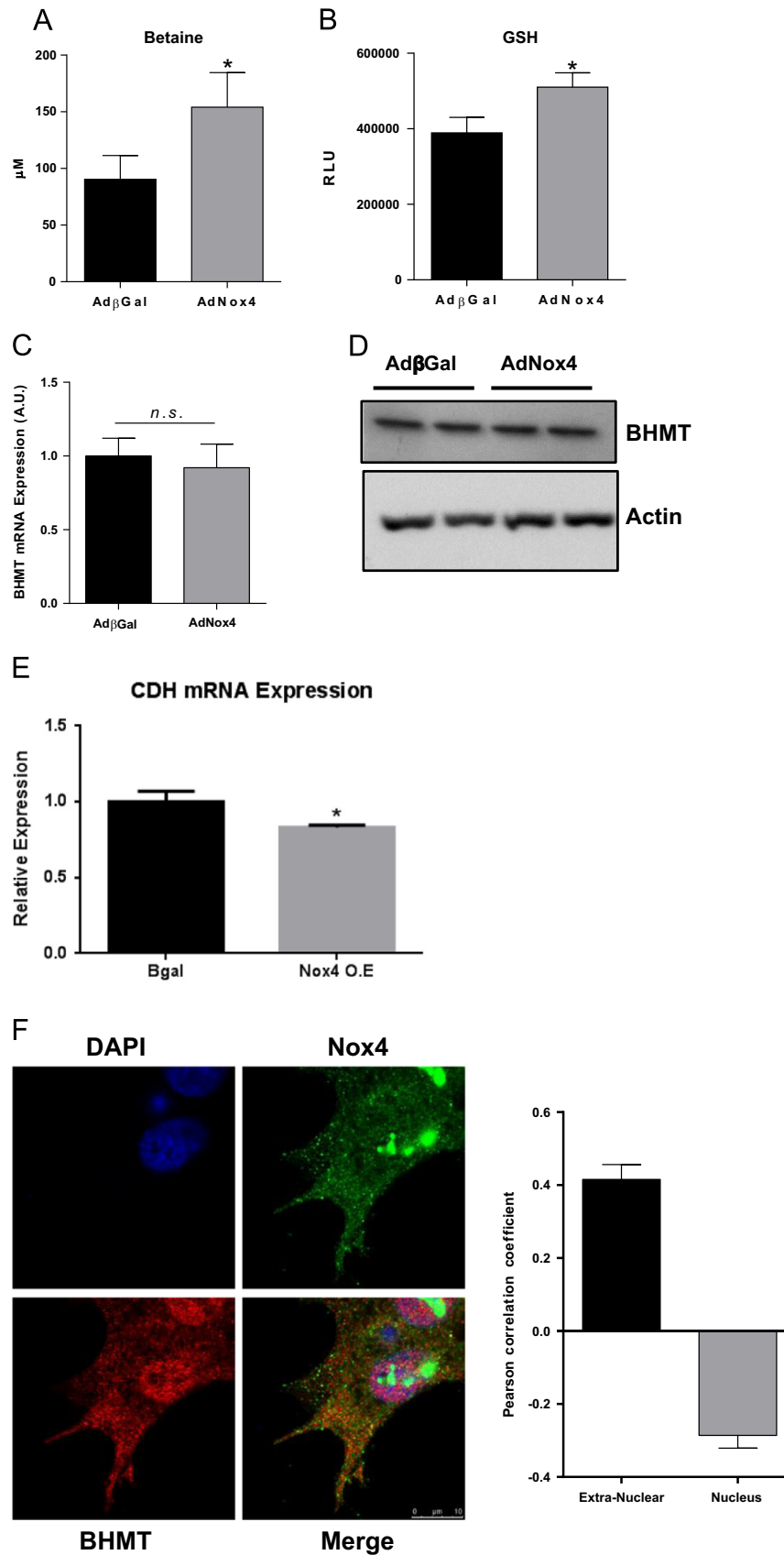
Fig. 7. *Nox4 overexpression increases betaine and GSH levels in HepG2 cells in vitro.*A, Betaine levels and B, GSH levels in HepG2 cells transduced with AdNox4 or control, AdβGal (n=6). C, mRNA levels of BHMT, normalised to βactin in HepG2 cells transduced with AdNox4 or control, AdβGal (n=3).D, Western blot analysis of BHMT protein levels in HepG2 cells transduced with AdNox4 or control AdβGal. E, mRNA levels of CDH, normalised to βactin in HepG2 cells transduced with AdNox4 or control, AdβGal (n=3). F, Representative confocal microscopy images of HepG2 stained with DAPI (blue), Nox4(green) and BHMT(red) and histograms showing Pearson's coefficients calculated for co-localization of Nox4 and BHMT in nuclear and extra-nuclear cellular compartments. The coefficient can vary between -1 and +1, with negative values representing inverse correlations, zero representing no co-localization, and +1 representing perfect co-localization. Above data are represented as mean +/-S.E.M. *: p= < 0.05. n.s.: not significant.
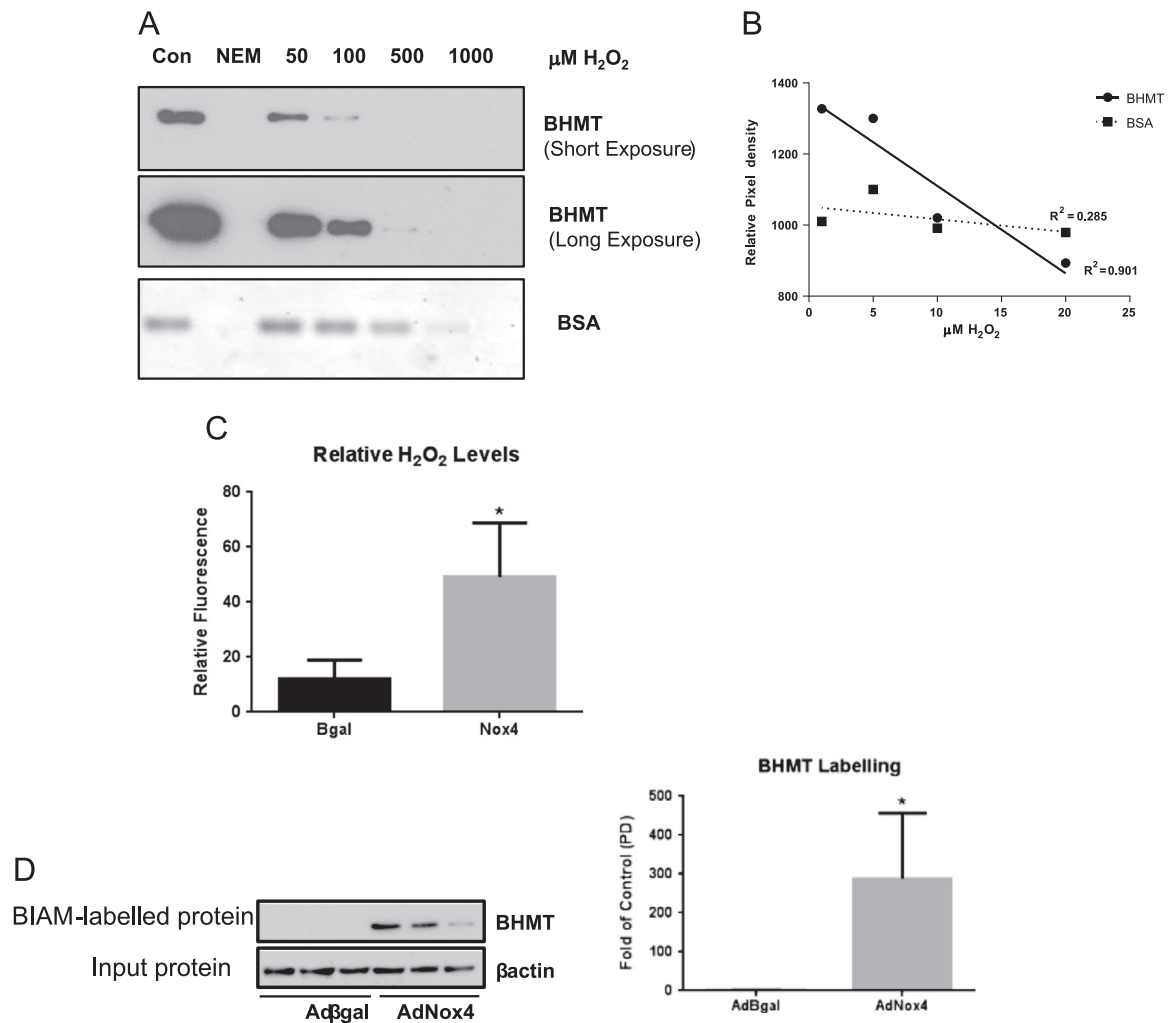
Fig. 8. *BHMT is a potential direct oxidative-target of Nox4-generated ROS.*A, Representative immunoblot showing decreasing labelling of BHMT after BIAM labelling of H_2O_2-oxidised purified recombinant BHMT and BSA. B, Graph of the densitometric analysis of labelled BHMT band intensities under the indicated H_2O_2 concentrations. R^2 values indicate that there is a good correlation between the decreases in BHMT labelling and increasing H_2O_2 concentration (i.e. increasingly oxidised BHMT), while there is a poor correlation between BSA labelling at the same H_2O_2 concentrations. C, Extracellular catalase-inhibitable H2O2 generated by HepG2 cells transduced with AdNox4 or control, AdβGal (n=3). D, Western blot and densitometric quanrification of BIAM-switch labelled (ie oxidised) BHMT levels in HepG2 cells transduced with AdNox4 or control, AdβGal (n=3). Equivalent amounts (20μg) of "input" protein were blotted for βactin, to serve as a control. Above data are represented as mean $+/-$S.E. M. *: p= < 0.05. n.s.: not significant.

dependent control, and that Nox4-generated ROS is a critical effector of this regulation. Remethylation pathways are potentially inhibited *in vivo* by pro-oxidants, due to known redox modifications of critical enzymes [23]. Consistent with this, we found evidence for increased activity of BHMT in the (less ROS-producing) Nox4$^{-/-}$ mice. Thus betaine levels, together with the ratio of betaine:DMG were both significantly reduced in the livers of Nox4$^{-/-}$ mice, indicating increased BHMT activity. Experiments in a human hepatocyte cell line (HepG2) complement these *in vivo* findings: Nox4 overexpression in HepG2 cells acted to *increase* the baseline intracellular concentrations of both betaine and GSH, consistent with *reduced* BHMT activity. These experiments further suggest that redox-regulation of BHMT activity may represent a conserved mechanism among mammalian species to direct Hcy partitioning to either methionine or cysteine pools.

We hypothesise that the regulation of BHMT by Nox4 is likely to be based on the 'redox switch' mechanism proposed by its crystal structure. Under reducing (activating) conditions a catalytic zinc ion is coordinated at the active site of BHMT by three cysteines (Cys 217, 299, 300). Oxidation promotes an intramolecular disulphide bond between Cys217 and Cys299 resulting in the displacement of the zinc ion, and enzyme inactivation [10]. A

similar mechanism by which Nox4-generated ROS inhibits the activity of protein-tyrosine-phosphatase 1B through the oxidation of critical active site cysteines has also been described [11,50], suggesting a conserved mechanism for redox-mediated enzyme inactivation. Consistent with this, we demonstrate here that H_2O_2 (the product of Nox4) is able to oxidise thiol groups of purified BHMT in a dose-dependent manner at physiological concentrations, while overexpression of Nox4 in HepG2 cells resulted in both increased H_2O_2 production, and clear oxidation of BHMT. Furthermore, analyses in HepG2 cells demonstrated that Nox4 and BHMT co-localise within non-nuclear compartment(s) potentially to enable direct redox-regulation of BHMT by Nox4-generated H_2O_2.

We thus propose that under normal physiological conditions *in vivo*, ROS generated by Nox4 acts as a negative regulator of BHMT activity. Hence ablation of Nox4 results in hyperactivation of BHMT and a higher rate of Hcy flux through this remethylation pathway, resulting in lower plasma Hcy levels and a reduced metabolic flux to cysteine. The potential clinical significance of misregulated BHMT is becoming increasingly clear. Deletion of BHMT in mice, which results in greatly increased plasma Hcy and hepatic betaine, renders these animals susceptible to fatty liver

and hepatocellular carcinomas [48]. By contrast the Zucker Diabetic Fatty rat model of type 2 diabetes is characterised, at early stages, by increased levels of expression of BHMT that correlate with significantly reduced levels of hepatic betaine and plasma homocysteine [52].

As a consequence of lowered hepatic cysteine levels, Nox4$^{-/-}$ mice display impaired hepatic GSH production. GSH is the most important and most abundant cellular redox buffer, and consequently depletion of GSH stores has been shown to render cells more susceptible to an oxidant insult. Hepatic GSH insufficiency in Nox4$^{-/-}$ mice leads to a markedly increased susceptibility to APAP-induced liver toxicity. APAP is metabolised by the cytochrome P450 enzymes to the highly reactive compound N-acetly-*p*-benzoquinone imine (NAPQI). One of the primary mechanisms of detoxifying NAPQI is through the production of an APAP-GSH conjugate [18]. The ingestion of large doses of APAP therefore leads to a substantial depletion of hepatic GSH, and clinical treatment of APAP-induced liver damage is administration of a large dose of NAC to help restore GSH levels [20]. The increased APAP-induced liver damage in the Nox4$^{-/-}$ mice was fully rescued by oral administration of NAC as a source of cysteine, confirming that the reduced production of cysteine (and as a consequence, of GSH) in these mice was the cause of the phenotype. Lower baseline hepatic GSH levels are also likely to render these mice more susceptible to other hepatotoxic stimuli (in addition to APAP), as well as to diseases in which lower GSH levels are known to be causative of disease progression. For example non-alcohol fatty liver disease, fibrosis, hepatocellular carcinoma, hepatitis and cirrhosis have all been linked with decreased antioxidant capacity [5]. In addition, hepatic GSH represents the major systemic store which can be mobilised as required to supply other physiological systems [25]. Low systemic GSH levels have also been implicated in a wide array of pathologies such as cardiovascular diseases [26], neurodegenerative diseases[30], diabetes [41], and cancer [45], in addition to developmental disorders such as congenital heart defects [19].

It may, however, seem counter-intuitive for the relative levels of reduced GSH levels to *decrease* in the absence of an oxidant (Nox4) as described here. Moreover in a previous study, in which Nox4 was ectopically overexpressed in cardiomyocytes, we intriguingly observed a converse *increase* in reduced GSH within the heart. In that case the cardiac-specific overexpression of Nox4 was demonstrated to upregulate the Nrf2 antioxidant response, which in turn promoted the expression of the GSH biosynthetic and recycling enzymes [6]. We found no evidence for the involvement of Nrf2 in the Nox4-dependent phenotype described here (thus Nrf2$^{-/-}$ mice did not display altered hepatic GSH levels; data not shown). None-the-less, both these experiments highlight the danger in the assumption that increased oxidant expression will necessarily result in a more oxidised cellular redox state, as is often made.

In conclusion, we demonstrate a physiological role of Nox4 in regulating the partitioning of Hcy flux to the remethylation and transsulfuration pathways by the redox-dependent regulation of BHMT activity. As a consequence of Nox4 deficiency, hepatic GSH stores become depleted, with clear profound clinical implications for both hepatic and systemic health.

Acknowledgements

References

[1] N. Anilkumar, G. San Jose, I. Sawyer, C.X. Santos, C. Sand, A.C. Brewer, D. Warren, A.M. Shah, A 28-kDa splice variant of NADPH oxidase-4 is nuclear-localized and involved in redox signaling in vascular cells, Arteriosclerosis, thrombosis, and vascular biology 33 (2013) e104–e112.

[2] N. Anilkumar, R. Weber, M. Zhang, A. Brewer, A.M. Shah, Nox4 and nox2 NADPH oxidases mediate distinct cellular redox signaling responses to agonist stimulation, Arteriosclerosis, thrombosis, and vascular biology 28 (2008) 1347–1354.

[3] A. Babelova, D. Avaniadi, O. Jung, C. Fork, J. Beckmann, J. Kosowski, N. Weissmann, N. Anilkumar, A.M. Shah, L. Schaefer, et al., Role of Nox4 in murine models of kidney disease, Free radical biology & medicine 53 (2012) 842–853.

[4] K. Bedard, K.H. Krause, The NOX family of ROS-generating NADPH oxidases: physiology and pathophysiology, Physiological reviews 87 (2007) 245–313.

[5] F. Bellanti, J. Sastre, G. Serviddio, Reactive Oxygen Species (ROS) and Liver Disease Therapy, in: I. Laher (Ed.), In Systems Biology of Free Radicals and Antioxidants, Springer, Berlin Heidelberg, 2014, pp. 1809–1838.

[6] A.C. Brewer, T.V. Murray, M. Arno, M. Zhang, N.P. Anilkumar, G.E. Mann, A. M. Shah, Nox4 regulates Nrf2 and glutathione redox in cardiomyocytes in vivo, Free radical biology & medicine 51 (2011) 205–215.

[7] J.M. Burgoon, J. Selhub, M. Nadeau, T.W. Sadler, Investigation of the effects of folate deficiency on embryonic development through the establishment of a folate deficient mouse model, Teratology 65 (2002) 219–227.

[8] J.R. Burgoyne, P. Eaton, A rapid approach for the detection, quantification, and discovery of novel sulfenic acid or S-nitrosothiol modified proteins using a biotin-switch method, Methods in enzymology 473 (2010) 281–303.

[9] J.R. Burgoyne, S. Oka, N. Ale-Agha, P. Eaton, Hydrogen peroxide sensing and signaling by protein kinases in the cardiovascular system, Antioxidants & redox signaling 18 (2013) 1042–1052.

[10] C. Castro, N.S. Millian, T.A. Garrow, Liver betaine-homocysteine S-methyltransferase activity undergoes a redox switch at the active site zinc, Archives of biochemistry and biophysics 472 (2008) 26–33.

[11] K. Chen, M.T. Kirber, H. Xiao, Y. Yang, J.F. Keaney Jr., Regulation of ROS signal transduction by NADPH oxidase 4 localization, The Journal of cell biology 181 (2008) 1129–1139.

[12] T.W. Chew, X. Jiang, J. Yan, W. Wang, A.L. Lusa, B.J. Carrier, A.A. West, O. V. Malysheva, J.T. Brenna, J.F. Gregory 3rd, et al., Folate intake, MTHFR genotype, and sex modulate choline metabolism in mice, The Journal of nutrition 141 (2011) 1475–1481.

[13] S. Fernandez-Roig, P. Cavalle-Busquets, J.D. Fernandez-Ballart, M. Ballesteros, M.I. Berrocal-Zaragoza, J. Salat-Batlle, P.M. Ueland, M.M. Murphy, Low folate status enhances pregnancy changes in plasma betaine and dimethylglycine concentrations and the association between betaine and homocysteine, The American journal of clinical nutrition 97 (2013) 1252–1259.

[14] J.D. Finkelstein, Methionine metabolism in mammals, The Journal of nutritional biochemistry 1 (1990) 228–237.

[15] A.N. Friedman, A.G. Bostom, J. Selhub, A.S. Levey, I.H. Rosenberg, The kidney and homocysteine metabolism, Journal of the American Society of Nephrology: JASN 12 (2001) 2181–2189.

[16] M.K. Gaitonde, A spectrophotometric method for the direct determination of cysteine in the presence of other naturally occurring amino acids, The Biochemical journal 104 (1967) 627–633.

[17] M. Geiszt, J.B. Kopp, P. Varnai, T.L. Leto, Identification of renox, an NAD(P)H oxidase in kidney, Proceedings of the National Academy of Sciences of the United States of America 97 (2000) 8010–8014.

[18] J.A. Hinson, D.W. Roberts, L.P. James, Mechanisms of acetaminophen-induced liver necrosis, Handbook of experimental pharmacology (2010) 369–405.

[19] C.A. Hobbs, M.A. Cleves, W. Zhao, S. Melnyk, S.J. James, Congenital heart defects and maternal biomarkers of oxidative stress, The American journal of clinical nutrition 82 (2005) 598–604.

[20] M.J. Hodgman, A.R. Garrard, A review of acetaminophen poisoning, Critical care clinics 28 (2012) 499–516.

[21] S.M. Innis, D. Hasman, Evidence of choline depletion and reduced betaine and dimethylglycine with increased homocysteine in plasma of children with cystic fibrosis. The, Journal of nutrition 136 (2006) 2226–2231.

[22] H. Jaeschke, M.R. McGill, A. Ramachandran, Oxidant stress, mitochondria, and cell death mechanisms in drug-induced liver injury: lessons learned from acetaminophen hepatotoxicity, Drug metabolism reviews 44 (2012) 88–106.

[23] J. Joseph, J. Loscalzo, Methoxistasis: integrating the roles of homocysteine and folic acid in cardiovascular pathobiology, Nutrients 5 (2013) 3235–3256.

[24] J. Kuroda, T. Ago, S. Matsushima, P. Zhai, M.D. Schneider, J. Sadoshima, NADPH oxidase 4 (Nox4) is a major source of oxidative stress in the failing heart, Proceedings of the National Academy of Sciences of the United States of America 107 (2010) 15565–15570.

[25] B.H. Lauterburg, J.D. Adams, J.R. Mitchell, Hepatic glutathione homeostasis in the rat: efflux accounts for glutathione turnover, Hepatology 4 (1984) 586–590.

[26] J.A. Leopold, J. Loscalzo, Oxidative enzymopathies and vascular disease, Arteriosclerosis, thrombosis, and vascular biology 25 (2005) 1332–1340.

[27] D. Li, L. Pickell, Y. Liu, Q. Wu, J.S. Cohn, R. Rozen, Maternal methylenetetrahydrofolate reductase deficiency and low dietary folate lead to adverse reproductive outcomes and congenital heart defects in mice, The American journal of clinical nutrition 82 (2005) 188–195.

[28] S.C. Lu, Regulation of glutathione synthesis, Current topics in cellular regulation 36 (2000) 95–116.

[29] J. Lyons, A. Rauh-Pfeiffer, Y.M. Yu, X.M. Lu, D. Zurakowski, R.G. Tompkins, A. M. Ajami, V.R. Young, L. Castillo, Blood glutathione synthesis rates in healthy adults receiving a sulfur amino acid-free diet, Proceedings of the National Academy of Sciences of the United States of America 97 (2000) 5071–5076.

[30] H.L. Martin, P. Teismann, Glutathione–a review on its role and significance in Parkinson's disease, FASEB journal: official publication of the Federation of American Societies for Experimental Biology 23 (2009) 3263–3272.

[31] J.M. McCord, The evolution of free radicals and oxidative stress, The American journal of medicine 108 (2000) 652–659.

[32] D.O. McGregor, W.J. Dellow, M. Lever, P.M. George, R.A. Robson, S.T. Chambers, Dimethylglycine accumulates in uremia and predicts elevated plasma homocysteine concentrations, Kidney international 59 (2001) 2267–2272.

[33] E. Mosharov, M.R. Cranford, R. Banerjee, The quantitatively important relationship between homocysteine metabolism and glutathione synthesis by the transsulfuration pathway and its regulation by redox changes, Biochemistry 39 (2000) 13005–13011.

[34] T.V. Murray, I. Smyrnias, A.M. Shah, A.C. Brewer, NADPH oxidase 4 regulates cardiomyocyte differentiation via redox activation of c-Jun protein and the cis-regulation of GATA-4 gene transcription, The Journal of biological chemistry 288 (2013) 15745–15759.

[35] G. Pare, D.I. Chasman, A.N. Parker, R.R. Zee, A. Malarstig, U. Seedorf, R. Collins, H. Watkins, A. Hamsten, J.P. Miletich, et al., Novel associations of CPS1, MUT, NOX4, and DPEP1 with plasma homocysteine in a healthy population: a genome-wide evaluation of 13 974 participants in the Women's Genome Health Study, Circulation Cardiovascular genetics 2 (2009) 142–150.

[36] E.I. Park, T.A. Garrow, Interaction between dietary methionine and methyl donor intake on rat liver betaine-homocysteine methyltransferase gene expression and organization of the human gene, The Journal of biological chemistry 274 (1999) 7816–7824.

[37] L.A. Possamai, M.J. McPhail, A. Quaglia, V. Zingarelli, R.D. Abeles, R. Tidswell, Z. Puthucheary, J. Rawal, C.J. Karvellas, E.M. Leslie, et al., Character and temporal evolution of apoptosis in acetaminophen-induced acute liver failure∗, Critical care medicine 41 (2013) 2543–2550.

[38] R. Ray, C.E. Murdoch, M. Wang, C.X. Santos, M. Zhang, S. Alom-Ruiz, N. Anilkumar, A. Ouattara, A.C. Cave, S.J. Walker, et al., Endothelial Nox4 NADPH oxidase enhances vasodilatation and reduces blood pressure in vivo, Arteriosclerosis, thrombosis, and vascular biology 31 (2011) 1368–1376.

[39] M. Reid, F. Jahoor, Glutathione in disease, Current opinion in clinical nutrition and metabolic care 4 (2001) 65–71.

[40] K.L. Schalinske, A.L. Smazal, Homocysteine imbalance: a pathological metabolic marker, Adv Nutr 3 (2012) 755–762.

[41] R.V. Sekhar, S.V. McKay, S.G. Patel, A.P. Guthikonda, V.T. Reddy, A. Balasubramanyam, F. Jahoor, Glutathione synthesis is diminished in

[42] M. Sethuraman, M.E. McComb, T. Heibeck, C.E. Costello, R.A. Cohen, Isotope-coded affinity tag approach to identify and quantify oxidant-sensitive protein thiols, Molecular & cellular proteomics: MCP 3 (2004) 273–278.

[43] D. Shah, S. Sah, A. Wanchu, M.X. Wu, A. Bhatnagar, Altered redox state and apoptosis in the pathogenesis of systemic lupus erythematosus, Immunobiology 218 (2013) 620–627.

[44] K. Simpson, C.M. Hogaboam, S.L. Kunkel, D.J. Harrison, C. Bone-Larson, N. W. Lukacs, Stem cell factor attenuates liver damage in a murine model of acetaminophen-induced hepatic injury, Laboratory investigation; a journal of technical methods and pathology 83 (2003) 199–206.

[45] S. Singh, A.R. Khan, A.K. Gupta, Role of glutathione in cancer pathophysiology and therapeutic interventions, Journal of experimental therapeutics & oncology 9 (2012) 303–316.

[46] M.H. Stipanuk, J.E. Dominy, J.I. Lee, R.M. Coloso, Mammalian cysteine metabolism: New insights into regulation of cysteine metabolism, Journal of Nutrition 136 (2006) 1652s–1659s.

[47] I. Takac, K. Schroder, L. Zhang, B. Lardy, N. Anilkumar, J.D. Lambeth, A.M. Shah, F. Morel, R.P. Brandes, The E-loop is involved in hydrogen peroxide formation by the NADPH oxidase Nox4, The Journal of biological chemistry 286 (2011) 13304–13313.

[48] Y.W. Teng, M.G. Mehedint, T.A. Garrow, S.H. Zeisel, Deletion of betaine-homocysteine S-methyltransferase in mice perturbs choline and 1-carbon metabolism, resulting in fatty liver and hepatocellular carcinomas, The Journal of biological chemistry 286 (2011) 36258–36267.

[49] D.M. Townsend, K.D. Tew, H. Tapiero, The importance of glutathione in human disease, Biomedicine & pharmacotherapy=Biomedecine & pharmacotherapie 57 (2003) 145–155.

[50] T.H. Truong, K.S. Carroll, Redox regulation of epidermal growth factor receptor signaling through cysteine oxidation, Biochemistry 51 (2012) 9954–9965.

[51] V. Vitvitsky, S. Dayal, S. Stabler, Y. Zhou, H. Wang, S.R. Lentz, R. Banerjee, Perturbations in homocysteine-linked redox homeostasis in a murine model for hyperhomocysteinemia, American journal of physiology Regulatory, integrative and comparative physiology 287 (2004) R39–R46.

[52] E.P. Wijekoon, B. Hall, S. Ratnam, M.E. Brosnan, S.H. Zeisel, J.T. Brosnan, Homocysteine metabolism in ZDF (type 2) diabetic rats, Diabetes 54 (2005) 3245–3251.

[53] G. Wu, Y.Z. Fang, S. Yang, J.R. Lupton, N.D. Turner, Glutathione metabolism and its implications for health, The Journal of nutrition 134 (2004) 489–492.

[54] M. Zhang, A.C. Brewer, K. Schroder, C.X. Santos, D.J. Grieve, M. Wang, N. Anilkumar, B. Yu, X. Dong, S.J. Walker, et al., NADPH oxidase-4 mediates protection against chronic load-induced stress in mouse hearts by enhancing angiogenesis, Proceedings of the National Academy of Sciences of the United States of America 107 (2010) 18121–18126.

patients with uncontrolled diabetes and restored by dietary supplementation with cysteine and glycine, Diabetes care 34 (2011) 162–167.